International Journal of Electronics and Communication Engineering.
ISSN 0974-2166 Volume 5, Number 4 (2012), pp. 521-532

http://www.irphouse.com

Analysis of Longitudinal E-Plane Rectangular Waveguide Power Dividers/Combiners using Multiple cavity Modelling Technique

Debendra Kumar Panda[1] and Ajay Chakraborty[2]

[1] *Jawaharlal Institute of Technology, Borawan, Khargone, Madhya Pradesh, India.*
[2] *Birla Institute of Technology, Mesra, Ranchi,India.*
Corresponding author: Dr. Debendra Kumar Panda,
e-mail: debendrakumar.panda@gmail.com

Abstract

A method of moment based analysis of an E-plane rectangular using Multiple Cavity Modelling Technique (MCMT) waveguide power divider/combiner has been presented in this paper. This E-plane rectangular waveguide power divider/combiner is different from the family of tees. The output ports are in the same planes as the input which is an advantage for two dimensional phased array applications. Finally attempt has been made to improve the frequency response characteristic of the above mentioned waveguide circuit by inserting a shorting post. The proposed power divider has good agreement with the MCMT, CST microwave studio simulated data and measured data.

INTRODUCTION

Low cost, Low Profile two dimensional scanning phased array antennas have wide application in Low Earth Orbit, Middle Earth Orbit and Geostationary Earth Orbit satellite communication. Multi-port Power divider has already found wide applications in phased array techniques and for power amplification. Basic requirements for the considered class of beam forming networks are: Low losses in the operational frequency band, the high accuracy of power splitting (With necessary amplitude and phase distribution at the outputs). The E-plane and H-plane joint equal and unequal power dividers/combiners are important building blocks of beam forming networks of phased array antennas and for amplification purposes. Takeda, Ishida and Isoda [1] described a waveguide power divider using metallic septum.. Dittloff, Bornemann and Arndt [2] presented a computer aided design procedure for optimum E-plane or H-plane N-furcated waveguide power dividers. A rigorous design theory

for compact rectangular power dividers with unsymmetrical series E-plane T-junctions of suitably optimized different waveguide heights and distances was described by Arndt et al. [3]. Sanada, Fukui and Nogi [4, 5] proposed a waveguide type microwave power divider/combiner of double-ladder multiple-port structure and a travelling wave microwave power divider composed of reflection less dividing unit which is advantageous for its low insertion loss and high power capability. The algorithms and optimization of three compact microwave power dividers on the base of H-plane angular H_{qo}-mode exciters was presented by Kirilenko, Rud and Tkachenko [6]. Synthesis of three-way H-plane rectangular waveguide combiner/divider networks was described by Gardner and Ong [7]. The Waveguide combiner/divider network was analyzed with mode matching technique. Soroka et al. [8] also worked on multi-channel waveguide power dividers. Christopher and Sami [9] analyzed over-moded rectangular waveguide components for a multi-moded RF power distribution system. A novel effective waveguide multiport power divider for frequency-scanned antenna arrays was presented by Ryabchy [10]. Das and Chakraborty [11] analyzed a multiport waveguide power divider/combiner using MCMT. Various types of longitudinal H-plane power dividers are discussed using MCMT [12-17]. Das and Chakraborty analyzed an E-plane power divider/combiner using MCMT [11]. However the efficiency of this E-Plane power divider/combiner is not up to satisfaction. Effort has been made to improve the frequency response on inclusion of a shorting post to the structure.

In this paper, multiple cavity modelling technique is used to analyze new E-plane power dividers/combiners which are smaller in size till today. The technique involves in replacing all the apertures and discontinuities of the waveguide structures, with equivalent magnetic current densities so that the given structure can be analyzed using only magnetic field integral equation. Since only the magnetic currents present in the apertures are considered the methodology involves only solving simple magnetic integral equation rather than the complex integral equation involving both the electric and magnetic current densities. Compared with other methods there are several advantages of the present method. Firstly, all cavities are dealt with in a unified manner. In this algorithm, the only difference among different structures is their input parameters, and same routine can be used to analyze all structures. Secondly the fields at all the aperture or discontinuities can be obtained for analysis.

II. FORMULATION OF THEORY

Fig.1 shows a basic E-plane 1:2 power divider/combiner with shorting post and with its cavity modelling and details of region is shown in Fig. 2, which shows, the structures have 3 waveguide regions and 4 cavity regions. The interfacing apertures between different regions are replaced by equivalent magnetic current densities. The electric field at the aperture is assumed to be

$$\vec{E} = \hat{u}_x \sum_{p=1}^{M} E_{px} e_{px} + \hat{u}_y \sum_{p=1}^{M} E_{py} e_{py} \tag{1}$$

Where the basis function e_p (p=1, 2, 3…M) are defined by

$$e_p^{i,y} = \begin{cases} \sin\left\{\dfrac{p\pi}{2L}\left(x - x_w + L\right)\right\} & \text{for } \begin{matrix} x_w - L \le x \le x_w + L \\ y_w - W \le y \le y_w + W \end{matrix} \\ 0 & \text{elsewhere} \end{cases} \tag{2a}$$

$$e_p^{i,x} = \begin{cases} \sin\left\{\dfrac{p\pi}{2W}\left(y - y_w + W\right)\right\} & \text{for } \begin{matrix} x_w - L \le x \le x_w + L \\ y_w - W \le y \le y_w + W \end{matrix} \\ 0 & \text{elsewhere} \end{cases} \tag{2b}$$

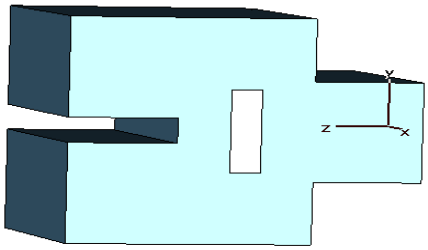

Fig. 1: Three dimensional view of an E-plane power divider/combiner with shorting post.

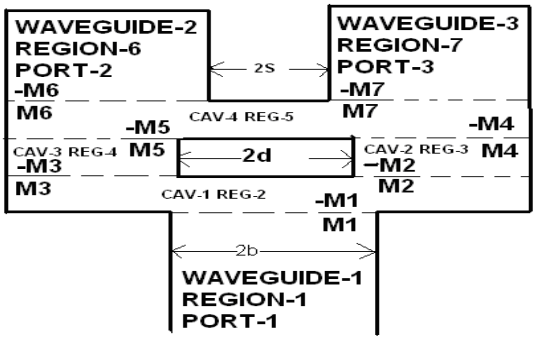

Fig. 2: Cavity modelling and details of regions of a basic E-plane power divider/combiner with shorting post.

In the eq. (2):

- $L = a, W = b$, $x_w = 0$ and $y_w = 0$ for aperture 1 with respect to cavity-1 axis.
- $L = a, W = (2b + s - d)/2$, $x_w = 0$ and $y_w = W + d$ for aperture 2 with respect to cavity-1 axis.
- $L = a, W = (2b + s - d)/2$, $x_w = 0$ and $y_w = -W - d$ for aperture 3 with respect to cavity-1 axis.
- $L = a, W = (2b + s - d)/2$, $x_w = 0$ and $y_w = 0$ for aperture 2 with respect to cavity-2 axis.
- $L = a, W = (2b + s - d)/2$, $x_w = 0$ and $y_w = 0$ for aperture 3 with respect to cavity-3 axis.

- $L = a, W = (2b + s - d)/2$, $x_w = 0$ and $y_w = 0$ for aperture 4with respect to cavity-2 axis.
- $L = a, W = (2b + s - d)/2$, $x_w = 0$ and $y_w = 0$ for aperture 5 with respect to cavity-3 axis.
- $L = a, W = (2b + s - d)/2$, $x_w = 0$ and $y_w = W + d$ for aperture 4 with respect to cavity-4 axis.
- $L = a, W = (2b + s - d)/2$, $x_w = 0$ and $y_w = -W - d$ for aperture 5 with respect to cavity-4 axis.
- $L = a, W = b$, $x_w = 0$ and $y_w = b + s$ for aperture 6 with respect to cavity-4 axis.
- $L = a, W = b$, $x_w = 0$ and $y_w = -b - s$ for aperture 7 with respect to cavity-4axis.

Where 2a=22.86mm, 2b=10.16mm, S=1.27mm and d=4.2mm.
Where 2s is the distance between waveguide-2 and waveguide-3.
2t=12.5mm is the cavity dimension of cavity.

The X-component of incident magnetic field at the aperture for the transmitting mode is a dominant TE_{10} mode and is given by $H_x^{inc} = -Y_0 \cos\left(\frac{\pi x}{2a}\right) e^{-j\beta z}$

III. EVALUATION OF THE CAVITY SCATTERED FIELD

The tangential components of the cavity scattered fields are given in [13] where L_{cj} the length is and W_{cj} is the height of j^{th} the cavity. L_i and W_i are the half length and half width of i^{th} aperture.

$$H_x^{cav^j}\left(M_i^x\right) = -\frac{j\omega\varepsilon}{k^2}\sum_{m=1}^{\infty}\sum_{n=0}^{\infty}\frac{\varepsilon_m\varepsilon_n L_i W_i}{2L_{cj}W_{cj}}\left\{k^2 - \left(\frac{m\pi}{2L_c}\right)^2\right\}\sin\left\{\frac{m\pi}{2L_{cj}}\left(x + L_{cj}\right)\right\}\times\cos\left\{\frac{n\pi}{2W_{cj}}\left(y + W_{cj}\right)\right\} \tag{9}$$
$$\cos\left\{\frac{n\pi}{2W_{cj}}\left(y_w + W_{cj}\right)\right\}\mathrm{sinc}\left\{\frac{n\pi}{2W_{cj}}W_i\right\}F_x(p)\times\frac{(-1)}{\Gamma_{mn}\sin\{2\Gamma_{mn}t_c\}}\begin{cases}\cos\{\Gamma_{mn}(z - t_c)\}\cos\{\Gamma_{mn}(z_0 + t_c)\} & z > z_0\\ \cos\{\Gamma_{mn}(z_0 - t_c)\}\cos\{\Gamma_{mn}(z + t_c)\} & z < z_0\end{cases}$$

$$H_x^{cav^j}\left(M_i^y\right) = \frac{j\omega\varepsilon}{k^2}\sum_{m=1}^{\infty}\sum_{n=0}^{\infty}\frac{\varepsilon_m\varepsilon_n L_i W_i}{2L_{cj}W_{cj}}\frac{m\pi}{2L_{cj}}\frac{n\pi}{2W_{cj}}\sin\left\{\frac{m\pi}{2L_{cj}}\left(x + L_{cj}\right)\right\}\times\cos\left\{\frac{n\pi}{2W_{cj}}\left(y + W_{cj}\right)\right\}\cos\left\{\frac{m\pi}{2L_{cj}}\left(x_w + L_{cj}\right)\right\} \tag{10}$$
$$\mathrm{sinc}\left\{\frac{m\pi}{2L_{cj}}L_i\right\}F_y(p)\times\frac{(-1)}{\Gamma_{mn}\sin\{2\Gamma_{mn}t_c\}}\begin{cases}\cos\{\Gamma_{mn}(z - t_c)\}\cos\{\Gamma_{mn}(z_0 + t_c)\} & z > z_0\\ \cos\{\Gamma_{mn}(z_0 - t_c)\}\cos\{\Gamma_{mn}(z + t_c)\} & z < z_0\end{cases}$$

$$H_y^{cav^j}\left(M_i^x\right) = \frac{j\omega\varepsilon}{k^2}\sum_{m=1}^{\infty}\sum_{n=0}^{\infty}\frac{\varepsilon_m\varepsilon_n L_i W_i}{2L_{cj}W_{cj}}\frac{m\pi}{2L_{cj}}\frac{n\pi}{2W_{cj}}\cos\left\{\frac{m\pi}{2L_{cj}}\left(x + L_{cj}\right)\right\}\times\sin\left\{\frac{n\pi}{2W_{cj}}\left(y + W_{cj}\right)\right\} \tag{11}$$
$$\cos\left\{\frac{n\pi}{2W_{cj}}\left(y_w + W_{cj}\right)\right\}\mathrm{sinc}\left\{\frac{n\pi}{2W_{cj}}W_i\right\}F_x(p)\times\frac{(-1)}{\Gamma_{mn}\sin\{2\Gamma_{mn}t_c\}}\begin{cases}\cos\{\Gamma_{mn}(z - t_c)\}\cos\{\Gamma_{mn}(z_0 + t_c)\} & z > z_0\\ \cos\{\Gamma_{mn}(z_0 - t_c)\}\cos\{\Gamma_{mn}(z + t_c)\} & z < z_0\end{cases}$$

$$H_y^{cav^j}\left(M_1^y\right)=-\frac{j\omega\varepsilon}{k^2}\sum_{m=1}^{\infty}\sum_{n=0}^{\infty}\frac{\varepsilon_m\varepsilon_n L_1 W_1}{2L_{cj}W_{cj}}\left\{k^2-\left(\frac{n\pi}{2W_{cj}}\right)^2\right\}\cos\left\{\frac{m\pi}{2L_{cj}}\left(x+L_{cj}\right)\right\}\times\sin\left\{\frac{n\pi}{2W_{cj}}\left(y+W_{cj}\right)\right\}\cos\left\{\frac{m\pi}{2L_{cj}}\left(x_w+L_{cj}\right)\right\} \quad (12)$$

$$\operatorname{sinc}\left\{\frac{m\pi}{2L_{cj}}L_1\right\}F_y(p)\times\frac{(-1)}{\Gamma_{mn}\sin\{2\Gamma_{mn}t_c\}}\begin{cases}\cos\{\Gamma_{mn}(z-t_c)\}\cos\{\Gamma_{mn}(z_0+t_c)\} & z>z_0\\ \cos\{\Gamma_{mn}(z_0-t_c)\}\cos\{\Gamma_{mn}(z+t_c)\} & z<z_0\end{cases}$$

Where t_c is half length of the cavity in z-direction and Γ_{mn} is the propagation constant

$$\Gamma_{mn}=\sqrt{k^2-\left(\frac{m\pi}{2l}\right)^2-\left(\frac{n\pi}{2w}\right)^2},\quad k=\omega\sqrt{\mu\varepsilon}\quad \varepsilon_i=\begin{cases}1, & i=0\\ 2, & i\neq 0\end{cases}$$

$$F_x(p)=\left[\cos\left\{\frac{\pi}{2}\left(-\frac{mx_w}{a_i}+p-m\right)\right\}\sin c\left\{\frac{\pi L}{2}\left(\frac{p}{L}-\frac{m}{a_i}\right)\right\}+\cos\left\{\frac{\pi}{2}\left(\frac{mx_w}{a_i}+p+m\right)\right\}\sin c\left\{\frac{\pi L}{2}\left(\frac{p}{L}+\frac{m}{a_i}\right)\right\}\right]$$

and

$$F_y(p)=\left[\cos\left\{\frac{\pi}{2}\left(-\frac{ny_w}{b_i}+p-n\right)\right\}\sin c\left\{\frac{\pi W}{2}\left(\frac{p}{W}-\frac{n}{b_i}\right)\right\}+\cos\left\{\frac{\pi}{2}\left(\frac{ny_w}{b_i}+p-n\right)\right\}\sin c\left\{\frac{\pi W}{2}\left(\frac{p}{W}+\frac{n}{b_i}\right)\right\}\right]$$

At the region of the window, the tangential component of the magnetic field in the aperture should be identical and applying the proper boundary conditions at the aperture the electric fields can be evaluated [6].

V. IMPOSITION OF THE BOUNDARY CONDITION

At the region of the window, the tangential component of the magnetic field in the aperture should be identical and is given by:

Aperture -1, Region-1

$$H_x^{wvg1}\left(M_1^x\right)+H_x^{cav1}\left(M_1^x\right)+H_x^{wvg1}\left(M_1^y\right)+H_x^{cav1}\left(M_1^y\right)-H_x^{cav1}\left(M_2^x\right)-H_x^{cav1}\left(M_2^y\right)-H_x^{cav1}\left(M_3^x\right)-H_x^{cav1}\left(M_3^y\right)=2H_x^{inc} \quad (13)$$

$$H_y^{wvg1}\left(M_1^x\right)+H_y^{cav1}\left(M_1^x\right)+H_y^{wvg1}\left(M_1^y\right)+H_y^{cav1}\left(M_1^y\right)-H_y^{cav1}\left(M_2^x\right)-H_y^{cav1}\left(M_2^y\right)-H_y^{cav1}\left(M_3^x\right)-H_y^{cav1}\left(M_3^y\right)=0 \quad (14)$$

Aperture -2, Region-2

$$-H_x^{cav1}\left(M_1^x\right)-H_x^{cav1}\left(M_1^y\right)+H_x^{cav1}\left(M_2^x\right)+H_x^{cav2}\left(M_2^x\right)+H_x^{cav1}\left(M_2^y\right)+H_x^{cav2}\left(M_2^y\right)+H_x^{cav1}\left(M_3^x\right)+H_x^{cav1}\left(M_3^y\right)-H_x^{cav2}\left(M_4^x\right)-H_x^{cav2}\left(M_4^y\right)=0 \quad (15)$$

$$-H_y^{cav1}\left(M_1^x\right)-H_y^{cav1}\left(M_1^y\right)+H_y^{cav1}\left(M_2^x\right)+H_y^{cav2}\left(M_2^x\right)+H_y^{cav1}\left(M_2^y\right)+H_y^{cav2}\left(M_2^y\right)+H_y^{cav1}\left(M_3^x\right)+H_y^{cav1}\left(M_3^y\right)-H_y^{cav2}\left(M_4^x\right)-H_y^{cav2}\left(M_4^y\right)=0 \quad (16)$$

Aperture -3, Region-2

$$-H_x^{cav1}\left(M_1^x\right)-H_x^{cav1}\left(M_1^y\right)+H_x^{cav1}\left(M_2^x\right)+H_x^{cav1}\left(M_2^y\right)+H_x^{cav1}\left(M_3^x\right)+H_x^{cav3}\left(M_3^x\right)+H_x^{cav1}\left(M_3^y\right)+H_x^{cav3}\left(M_3^y\right)-H_x^{cav3}\left(M_5^x\right)-H_x^{cav3}\left(M_5^y\right)=0 \quad (17)$$

$$-H_y^{cav1}\left(M_1^x\right)-H_y^{cav1}\left(M_1^y\right)+H_y^{cav1}\left(M_2^x\right)+H_y^{cav1}\left(M_2^y\right)+H_y^{cav1}\left(M_3^x\right)+H_y^{cav3}\left(M_3^x\right)+H_y^{cav1}\left(M_3^y\right)+H_y^{cav3}\left(M_3^y\right)-H_y^{cav3}\left(M_5^x\right)-H_y^{cav3}\left(M_5^y\right)=0 \quad (18)$$

Aperture -4, Region-3

$$-H_x^{an2}(M_1)-H_x^{an2}(M_2)+H_x^{an2}(M_4)+H_x^{an4}(M_4)+H_x^{an2}(M_4)+H_x^{an4}(M_4)+H_x^{an4}(M_5)+H_x^{an4}(M_5)-H_x^{an4}(M_6)+H_x^{an4}(M_6)-H_x^{an4}(M_7)+H_x^{an4}(M_7)=0 \quad (19)$$

$$-H_y^{an2}(M_1)-H_y^{an2}(M_2)+H_y^{an2}(M_4)+H_y^{an4}(M_4)+H_y^{an2}(M_4)+H_y^{an4}(M_4)+H_y^{an4}(M_5)+H_y^{an4}(M_5)-H_y^{an4}(M_6)+H_y^{an4}(M_6)-H_y^{an4}(M_7)+H_y^{an4}(M_7)=0 \quad (20)$$

Aperture -5, Region-4

$$-H_x^{an3}(M_3)-H_x^{an3}(M_3)+H_x^{an3}(M_5)+H_x^{an4}(M_5)+H_x^{an3}(M_5)+H_x^{an4}(M_5)+H_x^{an4}(M_4)+H_x^{an4}(M_4)-H_x^{an4}(M_6)+H_x^{an4}(M_6)-H_x^{an4}(M_7)+H_x^{an4}(M_7)=0 \quad (21)$$

$$-H_y^{cav3}(M_3^x)-H_y^{cav3}(M_3^y)+H_y^{cav3}(M_5^x)+H_y^{cav4}(M_5^x)+H_y^{cav3}(M_5^y)+H_y^{cav4}(M_5^y)+ H_y^{cav4}(M_4^x)+H_y^{cav4}(M_4^y)-H_y^{cav4}(M_6^x)-H_y^{cav4}(M_6^y)-H_y^{cav4}(M_7^x)-H_y^{cav4}(M_7^y)=0 \quad (22)$$

Aperture -6, Region-5

$$-H_x^{an4}(M_4)-H_x^{an4}(M_4)-H_x^{an4}(M_5)-H_x^{an4}(M_5)+H_x^{wav2}(M_6)+H_x^{wav-2}(M_6)+H_x^{an4}(M_6)+H_x^{an4}(M_7)+H_x^{an4}(M_7)=0 \quad (23)$$

$$-H_y^{an4}(M_4)-H_y^{an4}(M_4)-H_y^{an4}(M_5)-H_y^{an4}(M_5)+H_y^{wav2}(M_6)+H_y^{wav-2}(M_6)+H_y^{an4}(M_6)+H_y^{an4}(M_7)+H_y^{an4}(M_7)=0 \quad (24)$$

Aperture -7, Region-5

$$-H_x^{can4}(M_4^x)-H_x^{can4}(M_4^y)-H_x^{can4}(M_5^x)-H_x^{can4}(M_5^y)+H_x^{wav3}(M_7^x)+H_x^{wav-3}(M_7^y)+H_x^{can4}(M_6^x)+H_x^{can4}(M_6^y)+H_x^{can4}(M_7^x)+H_x^{can4}(M_7^y)=0 \quad (25)$$

$$-H_y^{can4}(M_4^x)-H_y^{can4}(M_4^y)-H_y^{can4}(M_5^x)-H_y^{can4}(M_5^y)+H_y^{wav3}(M_7^x)+H_y^{wav3}(M_7^y)+H_y^{can4}(M_6^x)+H_y^{can4}(M_6^y)+H_y^{can4}(M_7^x)+H_y^{can4}(M_7^y)=0 \quad (26)$$

VI. SOLVING FOR THE ELECTRIC FIELD

To determine the electric field distribution at the window aperture, it is necessary to determine the basis function coefficients $E_p^{i,x/y}$ at both the apertures. Since the each component of the field is described by M basis functions, 14M unknowns are to be determined from the boundary conditions. The Galerkin's specialization of the method of moments is used to obtain 14M-different equations from the boundary condition to enable determination of $E_p^{i,x/y}$ [10]. The weighting function $w_q^{i,x/y}(x,y,z)$ is selected to be of the same form as the basis function $e_p^{i,x/y}$. The weighting function is defined as follows:

$$w_q^{i,y}=\begin{cases}\sin\left\{\dfrac{q\pi}{2L}(x-x_w+L)\right\} & \text{for } \begin{matrix}x_w\text{-}L\le x\le x_w+L\\ y_w\text{-}W\le y\le y_w+W\end{matrix}\\ 0 & \text{elsewhere}\end{cases} \quad (27a)$$

$$w_q^{i,x}=\begin{cases}\sin\left\{\dfrac{q\pi}{2W}(y-y_w+W)\right\} & \text{for } \begin{matrix}x_w\text{-}L\le x\le x_w+L\\ y_w\text{-}W\le y\le y_w+W\end{matrix}\\ 0 & \text{elsewhere}\end{cases} \quad (27b)$$

The inner product is defined by

$$\langle H, w_q\rangle = \iint_{Aperture} H\,w_q\,d\xi\,d\psi \quad (28)$$

where the elements of the moment matrices are derived as follows:

$$\left\langle H_x^{inc}, w_q^{1,y} \right\rangle = \begin{cases} -2abY_0 & \text{for q = 1} \\ 0 & \text{otherwise} \end{cases} \tag{29}$$

$$\left\langle H_x^{wvg}(M_x), w_q^{i,y} \right\rangle = \begin{cases} -2abY_{m0}^{e} & \text{for p = q = m and n = 0} \\ 0 & \text{Otherwise} \end{cases} \tag{30}$$

$$\left\langle H_x^{wvg}(M_y), w_q^{i,y} \right\rangle = 0 \tag{31}$$

$$\left\langle H_y^{wvg}(M_x), w_q^{i,x} \right\rangle = 0 \tag{32}$$

$$\left\langle H_y^{wvg}(M_y), w_q^{i,x} \right\rangle = \begin{cases} -2abY_{0n}^{e} & \text{for p = q = n and m = 0} \\ 0 & \text{Otherwise} \end{cases} \tag{33}$$

$$\left\langle H_x^{cav}(M_x), w_q^{i,y} \right\rangle = -\frac{j\omega\varepsilon}{k^2}\frac{L_sW_sL_oW_o}{2L_cW_c}\sum_{m=1}^{\infty}\sum_{n=0}^{\infty}\varepsilon_m\varepsilon_n\left\{k^2-\left(\frac{m\pi}{2L_c}\right)^2\right\}\times\cos\left\{\frac{n\pi}{2W_c}(y_{ws}+W_c)\right\}\sin c\left\{\frac{n\pi}{2W_c}W_s\right\} \tag{34}$$
$$\cos\left\{\frac{n\pi}{2W_c}(y_{wo}+W_c)\right\}\sin c\left\{\frac{n\pi}{2W_c}W_o\right\}\times\frac{\{-F_{xs}(p)F_{xo}(q)\}}{\Gamma_{mn}\sin\{2\Gamma_{mn}t_c\}}\begin{cases}\cos\{\Gamma_{mn}(z-t_c)\}\cos\{\Gamma_{mn}(z_0+t_c)\} & z>z_0\\ \cos\{\Gamma_{mn}(z_0-t_c)\}\cos\{\Gamma_{mn}(z+t_c)\} & z<z_0\end{cases}$$

$$\left\langle H_x^{cav}(M_y), w_q^{i,y} \right\rangle = \frac{j\omega\varepsilon}{k^2}\frac{L_sW_sL_oW_o}{2L_cW_c}\sum_{m=0}^{\infty}\sum_{n=1}^{\infty}\varepsilon_m\varepsilon_n\frac{m\pi}{2L_c}\frac{n\pi}{2W_c}\times\cos\left\{\frac{m\pi}{2L_c}(x_{ws}+L_c)\right\}\sin c\left\{\frac{m\pi}{2L_c}L_s\right\} \tag{35}$$
$$\cos\left\{\frac{n\pi}{2W_c}(y_{wo}+W_c)\right\}\sin c\left\{\frac{n\pi}{2W_c}W_o\right\}\times\frac{\{-F_{ys}(p)F_{xo}(q)\}}{\Gamma_{mn}\sin\{2\Gamma_{mn}t_c\}}\begin{cases}\cos\{\Gamma_{mn}(z-t_c)\}\cos\{\Gamma_{mn}(z_0+t_c)\} & z>z_0\\ \cos\{\Gamma_{mn}(z_0-t_c)\}\cos\{\Gamma_{mn}(z+t_c)\} & z<z_0\end{cases}$$

$$\left\langle H_y^{cav}(M_x), w_q^{i,x} \right\rangle = \frac{j\omega\varepsilon}{k^2}\frac{L_sW_sL_oW_o}{2L_cW_c}\sum_{m=1}^{\infty}\sum_{n=0}^{\infty}\varepsilon_m\varepsilon_n\frac{m\pi}{2L_c}\frac{n\pi}{2W_c}\times\cos\left\{\frac{m\pi}{2L_c}(x_{wo}+L_c)\right\}\sin c\left\{\frac{m\pi}{2L_c}L_o\right\} \tag{36}$$
$$\cos\left\{\frac{n\pi}{2W_c}(y_{ws}+W_c)\right\}\sin c\left\{\frac{n\pi}{2W_c}W_s\right\}\times\frac{\{-F_{xs}(p)F_{yo}(q)\}}{\Gamma_{mn}\sin\{2\Gamma_{mn}t_c\}}\begin{cases}\cos\{\Gamma_{mn}(z-t_c)\}\cos\{\Gamma_{mn}(z_0+t_c)\} & z>z_0\\ \cos\{\Gamma_{mn}(z_0-t_c)\}\cos\{\Gamma_{mn}(z+t_c)\} & z<z_0\end{cases}$$

$$\left\langle H_y^{cav}(M_y), w_q^{i,x} \right\rangle = -\frac{j\omega\varepsilon}{k^2}\frac{L_sW_sL_oW_o}{2L_cW_c}\sum_{m=0}^{\infty}\sum_{n=1}^{\infty}\varepsilon_m\varepsilon_n\left\{k^2-\left(\frac{n\pi}{2W_c}\right)^2\right\}\times\cos\left\{\frac{m\pi}{2L_c}(x_{ws}+L_c)\right\}\sin c\left\{\frac{m\pi}{2L_c}L_s\right\} \tag{37}$$
$$\cos\left\{\frac{m\pi}{2L_c}(x_{wo}+L_c)\right\}\sin c\left\{\frac{m\pi}{2L_c}L_o\right\}\times\frac{\{-F_{ys}(p)F_{yo}(q)\}}{\Gamma_{mn}\sin\{2\Gamma_{mn}t_c\}}\begin{cases}\cos\{\Gamma_{mn}(z-t_c)\}\cos\{\Gamma_{mn}(z_0+t_c)\} & z>z_0\\ \cos\{\Gamma_{mn}(z_0-t_c)\}\cos\{\Gamma_{mn}(z+t_c)\} & z<z_0\end{cases}$$

where suffix 's' and 'o' represents the source and observation aperture dimensions respectively.

VII. REFLECTION COEFFICIENT AND TRANSMISSION COEFFICIENT

To determine the reflection coefficient, we decouple the sources, one at $-\infty$ in the feed waveguide and the other at the window. The incident electric field due to the TE_{10} excitation at the z = 0 plane is:

$$E_y^{inc} = \cos\left(\frac{\pi x}{2a_i}\right) \tag{38}$$

When the window aperture is shorted, the electric field is the field reflected by the electric short circuit and is given by,

$$E_y^{1} = -\cos\left(\frac{\pi x}{2a_i}\right) \tag{39}$$

When the generator in the feed waveguide is removed and replaced by a perfect match, the electric field for the dominant TE_{10} mode scattered by the window into the waveguide is derived from equation (9) by substituting m =1, n = 0, at the z = 0 plane

as:

$$E_y^2 = \sum_{p=1}^{M} E_p^{i,y} \frac{WL}{ab}\left[\cos\left\{\frac{\pi}{2}\left(-\frac{x_w}{a}+p+1\right)\right\}\sin c\left\{\frac{\pi L}{2}\left(\frac{p}{L}-\frac{1}{a}\right)\right\}-\cos\left\{\frac{\pi}{2}\left(\frac{x_w}{a}+p+1\right)\right\}\sin c\left\{\frac{\pi L}{2}\left(\frac{p}{L}+\frac{1}{a}\right)\right\}\right]\cos\left(\frac{\pi x}{2a}\right) \tag{40}$$

Reflection coefficient Γ can then be expressed as:

$$\Gamma = \frac{E_y^1 + E_y^2}{E_y^{inc}} = -1 + \frac{W_i L_i}{a_i b_i}\sum_{p=1}^{M} E_p^{i,y}\left[\cos\left\{\frac{\pi}{2}\left(-\frac{x_w}{a_i}+p+1\right)\right\}\sin c\left\{\frac{\pi L_i}{2}\left(\frac{p}{L_i}-\frac{1}{a_i}\right)\right\}-\cos\left\{\frac{\pi}{2}\left(\frac{x_w}{a_i}+p+1\right)\right\}\sin c\left\{\frac{\pi L_i}{2}\left(\frac{p}{L_i}+\frac{1}{a_i}\right)\right\}\right] \tag{41}$$

The transmission coefficient is given by

$$T_{ji} = \frac{E_y^{transmitted}}{E_y^{inc}} = \frac{W_j L_j}{a_j b_j}\sum_{p=1}^{M} E_p^{j,y}\left[\cos\left\{\frac{\pi}{2}\left(-\frac{x_w}{a_j}+p+1\right)\right\}\sin c\left\{\frac{\pi L_j}{2}\left(\frac{p}{L_j}-\frac{1}{a_j}\right)\right\}-\cos\left\{\frac{\pi}{2}\left(\frac{x_w}{a_j}+p+1\right)\right\}\sin c\left\{\frac{\pi L_j}{2}\left(\frac{p}{L_j}+\frac{1}{a_j}\right)\right\}\right] \tag{42}$$

The scattering matrix for this power divider/combiner is as follows:

$$\begin{pmatrix} S_{11} & S_{12} & S_{13} \\ S_{21} & S_{22} & S_{23} \\ S_{31} & S_{32} & S_{33} \end{pmatrix} \tag{43}$$

VIII. NUMERICAL RESULTS AND DISCUSSION

Theoretical data for the magnitude of scattering parameters for an E-plane WR-90 waveguide power divider/combiner without shorting post at X-band has been compared with CST Microwave Studio simulated data in Fig. 3-4, for the values of 2t=10mm,15mm,20mm and 25mm where 2t is the cavity dimension in Z-direction.

MATLAB codes have been written to analyze the structure Fig.1 and numerical data have been obtained after running the codes. The structure was also simulated using CST microwave studio while measurements were performed using Agilent 8410C Vector Network Analyzer. The theory has been validated by the excellent agreement between the CST Microwave Studio simulated data and Measured Data.

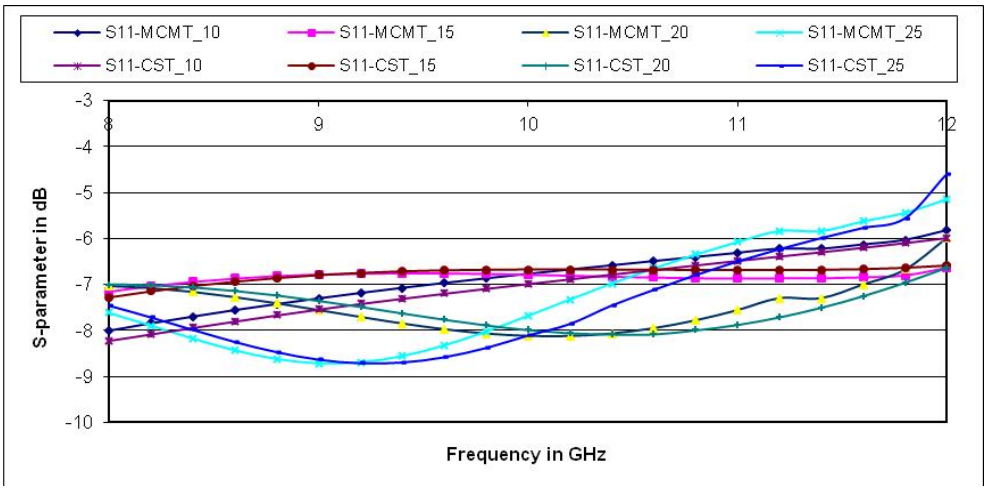

Fig. 3: Comparison of theoretical, CST Microwave Studio simulated data of S_{11} for an E-plane WR-90 waveguide power divider/combiner without shorting post for 2t=10mm, 15mm, 20mm and 25mm.

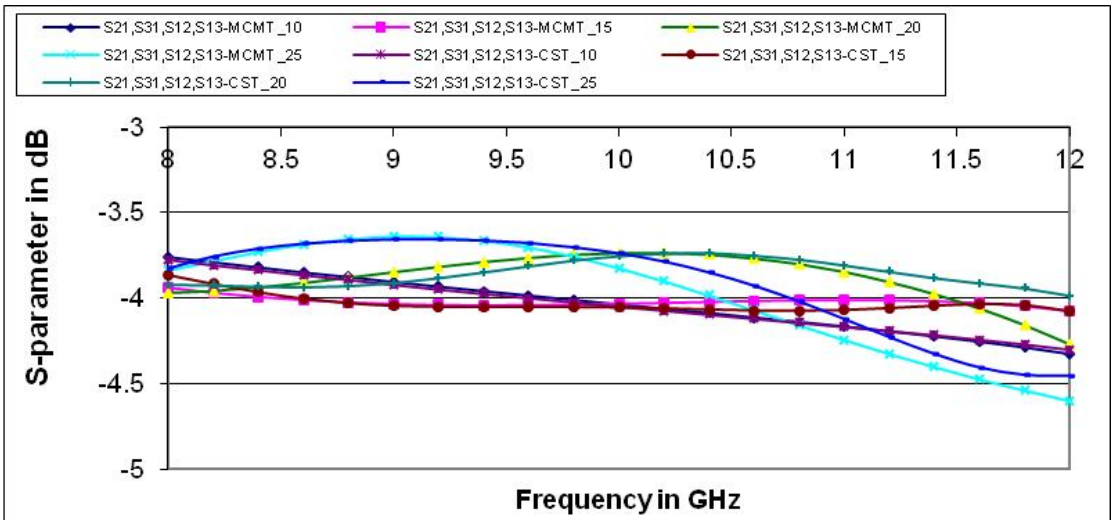

Figure 4: Comparison of theoretical, CST Microwave Studio simulated data of S-parameters for an E-plane WR-90 waveguide power divider/combiner without shorting post for 2t=10mm, 15mm, 20mm and 25mm.

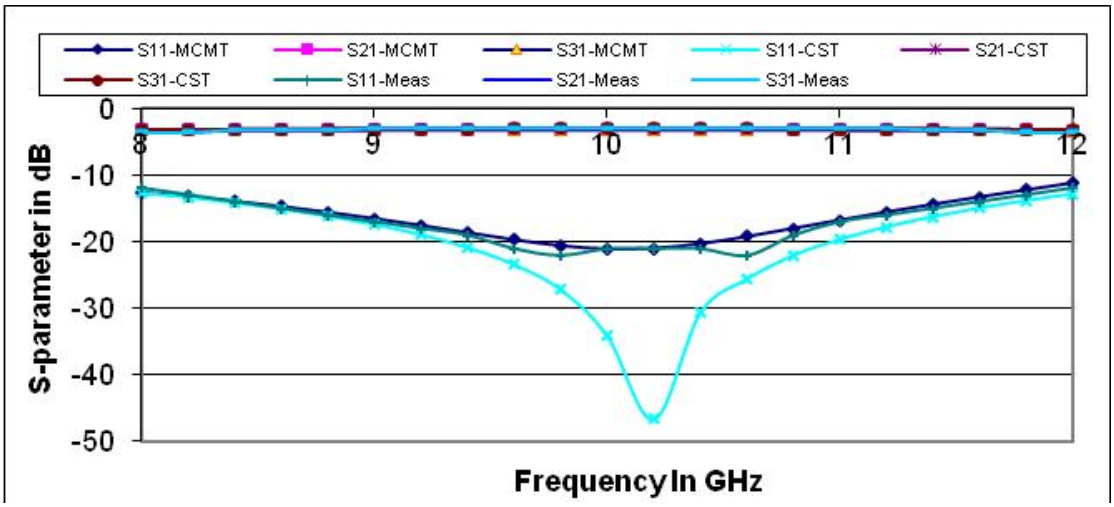

Fig. 5: Comparison of theoretical, CST Microwave Studio simulated and measured data of s-parameters for an E-plane WR-90 waveguide power divider/combiner with shorting post when excited at port-1 with 2t=12.5mm.

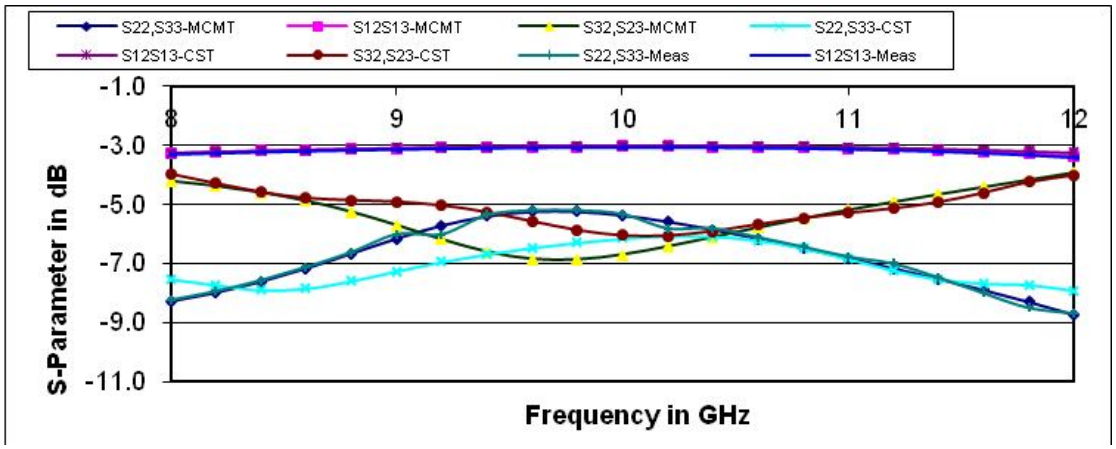

Fig. 6: Comparison of theoretical, CST Microwave Studio simulated and measured data of s-parameters for an E-plane WR-90 waveguide power divider/combiner with shorting post when excited at port-2 & 3 with 2t=12.5mm.

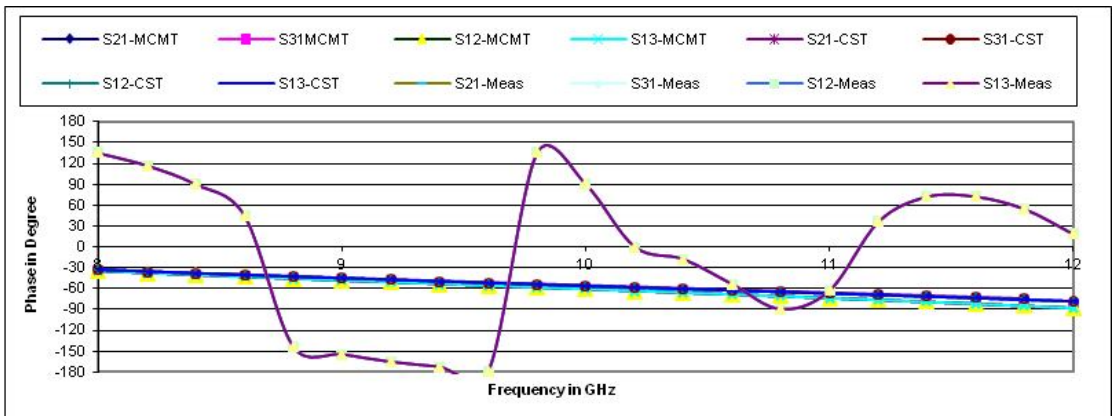

Fig. 7: Comparison of theoretical, CST Microwave Studio simulated and measured data for phase of s-parameters for an E-plane WR-90 waveguide power divider/combiner with 2t=12.5mm.

In Fig. 5-6 the magnitude of S-parameters for the proposed power divider/combiner with a shorting post have been shown, which shows that the $S_{21,}$ S_{31}, S_{12}, and S_{13} have the equal magnitude over the entire X-band. In Fig. 6, $S_{22,}$ $S_{33,}$ and S_{23}, S_{32} have the same magnitude over the entire X-band. In Fig. 7, the phase of the $S_{21,}$ $S_{12,}$ S_{13} and S_{31} have shown which shows that the phases of all these parameters are equal. The phase of S_{11}, $S_{22,}$ $S_{33,}$ S_{23} and S_{32} has not been presented in this context as these parameters are less important in the analysis of a power divider and combiner.

IX. CONCLUSION

From the above discussion it concludes that a longitudinal E-plane power divider/combiner is not matched to the junction. It requires proper matching which can be achieved by inserting a shorting post to the structure.

ACKNOWLEDGEMENT

The support provided by Kalpana Chawla Space Technology Cell, IIT Kharagpur is gratefully acknowledged.

REFERENCES

[1] Takeda. F., Ishida. O. and Isoda. Y., "Waveguide Power Divider Using Metallic Septum with Resistive Coupling Slot," Microwave Symposium Digest, MTT-S International, Vol. 82, Issue 1, pp. 527 – 528, June 1982.

[2] Dittloff, J., Bornemann, J. and Arndt, F., "Computer Aided Design of Optimum E- or H-Plane N-Furcated Waveguide Power Dividers" European Microwave Conference, 1987. pp.181 – 186, 17th Oct. 1987.

[3] Arndt F., Ahrens I., Papziner U., Wiechmann U. and Wilkeit R., Optimized E-plane T-Junction Series Power Dividers," IEEE Transactions on Microwave Theory and Techniques, Vol. 35, No. 11, pp. 1052-1059, November 1987.

[4] Sanada A., Fukui K., and Nogi S., "A Waveguide Type Power Divider/Combiner of Double-Ladder Multiple-Port Structure", IEEE Transactions on Microwave Theory and Techniques, Vol. 42, No. 7, pp.1154 - 1161 July. 1994.

[5] Sanada A., Fukui K., and Nogi S., "Traveling Wave Microwave Power Divider Composed of Reflectionless Dividing Units", IEEE Transactions on Microwave Theory and Techniques, Vol. 43, No. 1, pp.14 -20 January. 1995.

[6] Kirilenko, A. A., Rud L. A. And TkachenkoV. I., "Full wave Analysis and Optimization of Microwave Power Dividers Based on the Angled Bend H_{qo}-mode Exciters", 25th European Microwave Conference, 1995, pp. 733-736. October 1995.

[7] Gardner. P. and Ong. B. H., "Mode Matching Design of Three-way Waveguide Power Dividers," IEE Colloquium on Advances in Passive Microwave Components, pp. 5/1-5/4 , 22 May 1997.

[8] Soroka. A. S., Silin. A. O., Tkachenko. V. I. and Tsakanyan. I. S., "Simulation of Multichannel Waveguide Power Dividers," MSMW'98 Symposium Proceedings, Kharkov, Ukraine, pp. 634-635, 15-17 September, 1998.

[9] Christopher D. N. and Sami G. T., "Overmoded Rectangular Waveguide Components for a Multi-Moded RF Power Distribution System", Proceedings of EPAC 2000, Viena, pp. 318-320, 2000.

[10] Ryabchy V. D., "Design of Multiport Waveguide Power Divider for Antenna Array",5th International Conference on Antenna Theory and Techniques, Kyiv, Ukraine, pp. 478-479, 24-27 May 2005.

[11] Das. S. and Chakrabarty. A. and Chakraborty. A. "Analysis of Multiport Waveguide Power Divider / Combiner for Phased Array Application,", NCC 2007, Kanpur, India, 2007.
[12] Das S. "Analysis of Rectangular Waveguide Based Passive Devices and Antennas Using Multiple Cavity Modeling Technique", PhD Dissertation, Department of E and ECE, I.I.T. Kharagpur, India, 2007.
[13] Panda D. K. and Chakraborty A., "Analysis of an 1:2 Rectangular Waveguide Power Divider for Phased Array Application Using Multiple Cavity Modeling Technique", Proceedings in Progress In Electromagnetic Research Symposium, Cambridge, USA, pp361-368,2008.
[14] Panda D. K. and Chakraborty A., "Analysis of a Longitudinal Rectangular Waveguide Power Divider/Combiner Using Multiple Cavity Modeling Technique", Proceedings of International conferences on Industrial and Information system (ICIIS-2008), IEEE, IIT Kharagpur, (8-10 December 2008).
[15] Panda D. K. and Chakraborty A., "Analysis of Folded H-plane Tee Junction Using Multiple Cavity Modeling Technique", Proceedings of International conferences on Industrial and Information system (ICIIS-2008), IEEE, IIT Kharagpur, (8-10 December 2008).
[16] Panda D. K. and Chakraborty A., "Multiple Cavity Modeling Of A Feed Network For Two Dimensional Phased Array Application" , Progress In Electromagnetics Research Letters, Vol. 2, 135–140, 2008
[17] Das. S. and Chakraborty. A., "A Novel Modeling Technique to Solve a Class of Rectangular Waveguide Based Circuits and Radiators," Progress in Electromagnetic Research, MIT, USA, Vol. 61, pp. 231-252, May 2006.
[18] Harrington, R.F., "Time-Harmonic Electromagnetic Fields", McGraw-Hill Book Company, New York, 1961.
[19] Collins, R.E., "Field Theory of Guided Waves", IEEE Press, 1991.
[20] Harrington, R.F., "Field Computation by Moment Methods", Roger E. Krieger Publishing Company, USA.